John L. Volakis
ElectroScience Lab
Electrical Engineering Dept.
The Ohio State University
1320 Kinnear Rd.
Columbus, OH 43212
+1 (614) 292-5846 Tel.
+1 (614) 292-7297 (Fax)
volakis.1@osu.edu (email)

David B. Davidson
Dept. E&E Engineering
University of Stellencosch
Stellenbosch 7600, South Africa
(+27) 21 808 4458
(+27) 21 808 4981 (Fax)
davidson@ing.sun.ac.za (e-mail)

Foreword by the Editors

Method of Moment Galerkin formulations applied to surfaces can involve quite computationally expensive numerical integration to evaluate: It is not uncommon for MoM codes to spend more time filling that factoring (or otherwise solving) the matrices. This month's contribution is from the time of our co-Editor, John Volakis, at the University of Michigan. It considers the semi-analytic evaluation of these integrals for electromagnetically small devices, in particular, RF-MEMS switches, where the fields are essentially quasi-static. Such contributions on the "nitty-gritty" of efficient formulations and coding are always extremely welcome!

Comparison of Semi-Analytical Formulations and Gaussian-Quadrature Rules for Quasi-Static Double-Surface Potential Integrals

Zhongde Wang[1], John Volakis[2], Kazuhiro Saitou[3], and Katsuo Kurabayashi[4]

[1]Electrical & Computer Engineering Department, University of Michigan
Ann Arbor, MI 48109-2122 USA
Tel: +1 (734) 764-0500; Fax: +1 (734) 747-2106; E-mail: agewang@eecs.umich.edu

[2]ElectroScience Lab, Electrical Engineering Department, The Ohio State University
1320 Kinnear Rd., Columbus, OH 43212 USA
Tel: +1 (614) 292-5846; Fax: +1 (614) 292-7297; E-mail: volakis.1@osu.edu

[3]Mechanical Engineering Department, University of Michigan
3211 EECS, 2350 Hayward St., Ann Arbor, MI 48109-2125 USA
Tel: +1 (734) 763-0036; Fax: +1 (734) 647-3170; E-mail: kazu@umich.edu

[4]Mechanical Engineering Department, University of Michigan
2272 GG Brown Lab/2125, Ann Arbor, MI 48109-2125 USA
Tel: +1 (734) 615-5211; Fax: +1 (734) 647-3170; E-mail: katsuo@umich.edu

Abstract

This paper presents a comparison of a new semi-analytical expression with Gaussian-quadrature formulas for the quasi-static double-surface potential integrals arising in the boundary integral (BI) models of micron-size objects, such as RF-MEMS switches. The integrals considered are the quasi-static Green's functions for the scalar and vector potentials, with constant or

linear basis functions over triangular subdomains. The examples given illustrate that the new semi-analytical formulations can achieve significantly higher solution accuracy and are more efficient when compared to the Gaussian-quadrature formulas.

Keywords: Integration; electrostatic analysis; magnetostatics; Gaussian quadrature; potential integrals

1. Introduction

Evaluations of the integrals involving the Green's function kernel and its derivative are important in the numerical implementation of the electric-field integral equations (EFIE) [1-5]. Over the past decades, many approaches have been presented [1, 3, 5, 6, 8, 9] to handle double surface potential integrals, based on triangular basis functions. As an extension of [2] and [6], this paper presents a semi-analytical method for computing the quasi-static double surface potential integrals, arising in the boundary integral (BI) models of electrically very small objects and for static electromagnetic-field computation.

The present work is motivated by our recent effort to model RF-MEMS switches [7], the typical dimensions of which are 100-600 μm in length and 50-150 μm in width. At 2 GHz, these dimensions correspond to an electrical length of $\lambda/1500$ - $\lambda/250$ and a width of $\lambda/3000$ - $\lambda/1000$, and thus the exponential factor $e^{-\mu R}$ can be replaced by unity (the quasi-static approximation). In addition to modeling RF-MEMS switches, the method can also improve the efficiency and accuracy of the solution in static electromagnetic problems [3]. The convergence analyses of the numerical examples demonstrate that our presented semi-analytical method can achieve higher solution accuracy in less computational time than the conventional Gaussian-quadrature formulae.

2. Semi-Analytical Formulation

Using Galerkin's method and the basis function defined in [7], the quasi-static integrals required for the evaluation of the EFIE matrices have the form

$$I_1' = \int_T \underbrace{\int_{T'} \frac{1}{R} dT'}_{I_1(r)} dT \tag{1}$$

$$\bar{I}_2' = \int_T \underbrace{\int_{T'} \nabla\left(\frac{1}{R}\right) dT'}_{\bar{I}_2(r)} dT \tag{2}$$

$$I_3' = \int_T N_i(\bar{r}) \underbrace{\int_{T'} N_j(\bar{r}') \frac{1}{R} dT'}_{I_3(r)} dT \tag{3}$$

$$\bar{I}_4' = \int_T N_i(\bar{r}) \underbrace{\int_{T'} N_j(\bar{r}') \nabla\left(\frac{1}{R}\right) dT'}_{\bar{I}_4(r)} dT \tag{4}$$

where T and T' represent the areas modified by the source and observation triangles/patches [2-5]; $R = |\bar{r} - \bar{r}'|$ is the distance from the source point, $\bar{r}$, in T to an observation point $\bar{r}'$ in T'; and N_i is the linear (nodal) function equal to unity at the ith node and zero at the other two.

These double surface integrals are commonly evaluated numerically via Gaussian-quadrature rules. Our approach is to instead replace the inner integrants, $I_1(r)$, $\bar{I}_2(r)$, $I_3(r)$, and $\bar{I}_4(r)$, with their analytical expressions in [2] and [6], and thus reduce the double surface integrals over T and T' with a single surface integral over T. Since [5] and [8] provide analytical expressions of Equations (1)-(4) in the case of $T = T'$, our focus is on the case $T \neq T'$.

Figures 1a - 1c illustrate the coordinate transformations from the global Cartesian space (x, y, z) to the local reference spaces (u, v, w) and (u', v', w') for the observation and source triangles T and T', respectively. Their corresponding simplex spaces

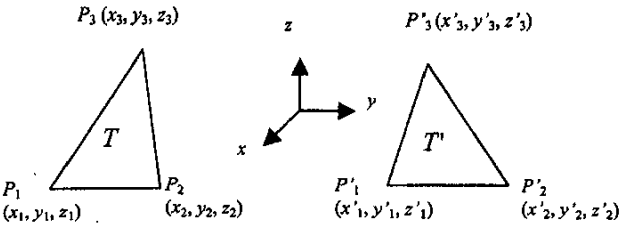

Figure 1a. The observation and source triangles, T and T', in global coordinates (x, y, z).

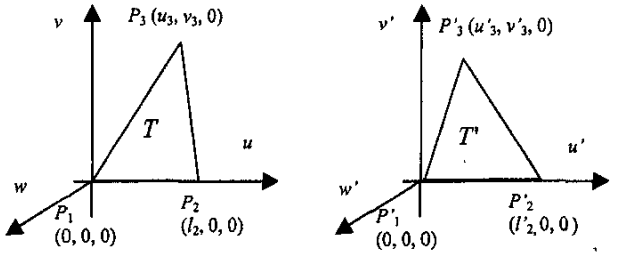

Figure 1b. The observation and source triangles, T and T', in local coordinates (u, v, w) and (u', v', w').

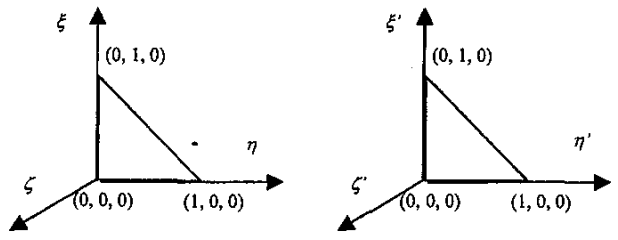

Figure 1c. The observation and source triangles, T and T', in simplex coordinates (η, ξ, ζ) and (η', ξ', ζ').

(η,ξ,ζ) and (η',ξ',ζ') are also shown. The transformation from (x,y,z) to (η,ξ,ζ) is given by

$$\begin{bmatrix} x \\ y \\ z \end{bmatrix} = \begin{bmatrix} x_1 & x_2 & x_3 \\ y_1 & y_2 & y_3 \\ z_1 & z_2 & z_3 \end{bmatrix} \begin{bmatrix} N_1(\eta,\xi) \\ N_2(\eta,\xi) \\ N_3(\eta,\xi) \end{bmatrix}, \tag{5}$$

where $N_1(\eta,\xi)$, $N_2(\eta,\xi)$, and $N_3(\eta,\xi)$ are the linear basic functions:

$$\begin{bmatrix} N_1(\eta,\xi) \\ N_2(\eta,\xi) \\ N_3(\eta,\xi) \end{bmatrix} = \begin{bmatrix} 1 & -1 & -1 \\ 0 & 1 & 0 \\ 0 & 0 & 1 \end{bmatrix} \begin{bmatrix} 1 \\ \eta \\ \xi \end{bmatrix}. \tag{6}$$

Also, the two-dimensional transformation from (u,v) to (η,ξ) is given by

$$\begin{bmatrix} \eta \\ \xi \end{bmatrix} = \frac{1}{2\Delta} \begin{bmatrix} v_3 & -u_3 \\ 0 & l_2 \end{bmatrix} \begin{bmatrix} u \\ v \end{bmatrix}, \tag{7}$$

where Δ is the area of triangle T. Corresponding transformations for the primed systems follow in a similar manner.

On replacing (x,y,z) with (η,ξ,ζ) and (η',ξ',ζ'), the integrals of Equations (1)-(4) take the form

$$I_1' = 2\Delta \int_0^1 \int_0^{1-\eta} I_1(\eta,\xi)\, d\xi d\eta, \tag{8}$$

$$\bar{I}_2' = 2\Delta \int_0^1 \int_0^{1-\eta} \bar{I}_2(\eta,\xi)\, d\xi d\eta, \tag{9}$$

$$I_3' = 2\Delta \int_0^1 \int_0^{1-\eta} N_i(\eta,\xi) I_3(\eta,\xi)\, d\xi d\eta, \tag{10}$$

$$\bar{I}_4' = 2\Delta \int_0^1 \int_0^{1-\eta} N_i(\eta,\xi) \bar{I}_4(\eta,\xi)\, d\xi d\eta, \tag{11}$$

where

$$I_1(\eta,\xi) = 2\Delta' \int_0^1 \int_0^{1-\eta'} \frac{1}{R}\, d\xi' d\eta', \tag{12}$$

$$\bar{I}_2(\eta,\xi) = 2\Delta' \int_0^1 \int_0^{1-\eta'} \nabla\left(\frac{1}{R}\right) d\xi' d\eta', \tag{13}$$

$$I_3(\eta,\xi) = 2\Delta' \int_0^1 \int_0^{1-\eta'} N_j'(\eta',\xi') \frac{1}{R}\, d\xi' d\eta', \tag{14}$$

$$\bar{I}_4(\eta,\xi) = 2\Delta' \int_0^1 \int_0^{1-\eta'} N_j'(\eta',\xi') \nabla\left(\frac{1}{R}\right) d\xi' d\eta'. \tag{15}$$

As mentioned earlier, of interest are the evaluations of I_1 to I_4 when R is very small, even for elements not sharing an edge. To address this issue, we chose here to evaluate the interior integral analytically, whereas the outer integral is evaluated using the standard Gaussian-quadrature approach. This is referred as our semi-analytical evaluation, and the extended analytical details are given in the appendix.

3. Comparison of Accuracy and Efficiency

This section compares the results of evaluating the four integrals in Equations (1)-(4) using the semi-analytical expressions of Equations (12)-(15), as compared to the direct Gaussian-quadrature evaluations. Based on a *FORTRAN* implementation of the two methods, the comparisons were made in terms of the computational time and the maximum relative error. From [9], it was determined that the Gaussian rule $G_{m,n}(m=n)$ was the best choice for balancing accuracy and computing time. In the following, the integrals were evaluated over a pair of edge-adjacent elements (Figure 2a) and a pair of node-adjacent elements (Figure 2b), with $i=j=1$ for I_3 and $\bar{I}_4$.

Figure 3 shows the comparison of the typical computational times for the four integrals in Equations (8)-(11). Clearly, the semi-analytic formulation saves time, especially as the number of integration points increases. For example, with $m=n=40$, the semi-analytical formulation required about 0.1 second, whereas

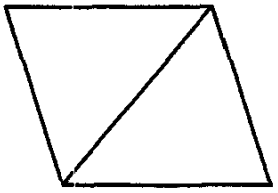

Figure 2a. Edge-adjacent elements.

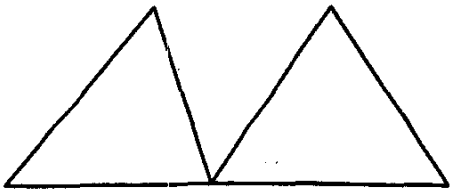

Figure 2b. Node-adjacent elements.

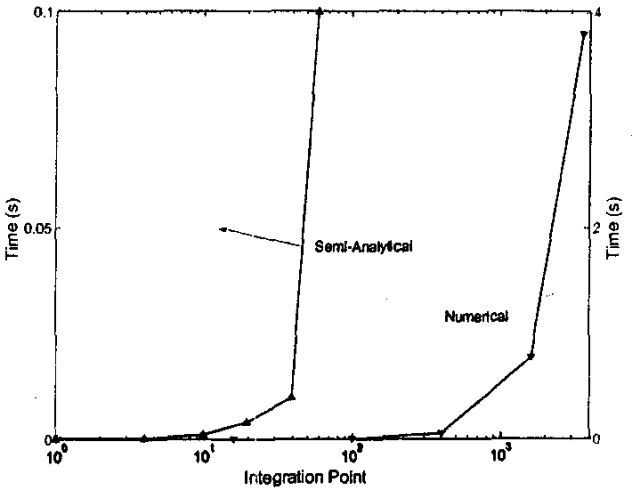

Figure 3. The computational time for the semi-analytical and Gaussian-quadrature $(m=n)$ expressions.

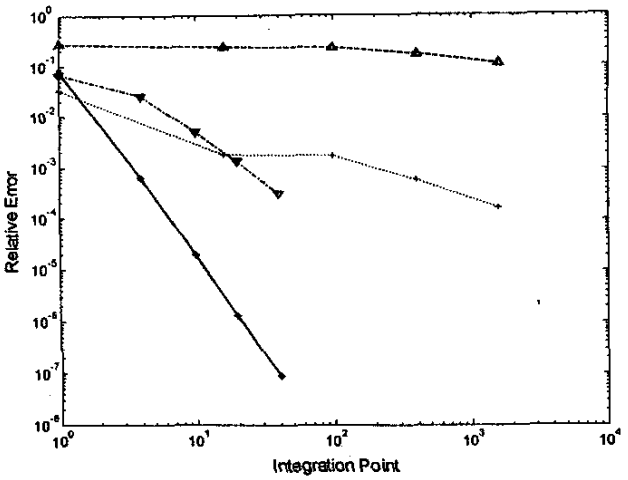

Figure 4a. The maximum relative error for the edge-adjacent elements I_1' and $\bar{I}_2'$. The dashed line is the Gaussian quadrature for I_1'; the dashed-doted line is the semi-analytical for I_1'; the doted line is the Gaussian quadrature for $\bar{I}_2'(1)$; the solid line is the semi-analytical for $\bar{I}_2'(1)$.

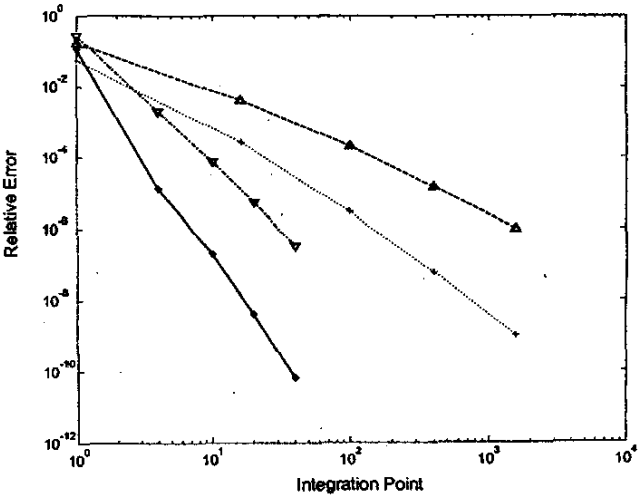

Figure 5a. The maximum relative error for the node-adjacent elements I_1' and $\bar{I}_2'$. The dashed line is the Gaussian quadrature for I_1'; the dashed-dotted line is the semi-analytical for I_1'; the dotted line is the Gaussian quadrature for $\bar{I}_2'(1)$; the solid line is the semi-analytical for $\bar{I}_2'(1)$.

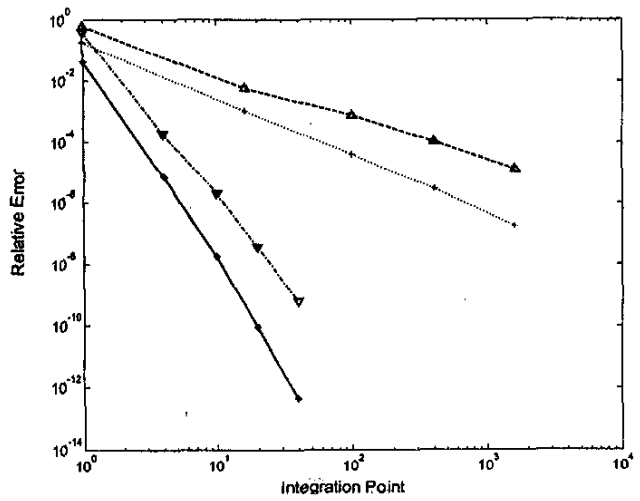

Figure 4b. The maximum relative error for the edge-adjacent elements I_3' and $\bar{I}_4'$. The dashed line is the Gaussian quadrature for I_3'; the dashed-dotted line is the semi-analytical for I_3'; The dotted line is the Gaussian quadrature for $\bar{I}_4'(1)$; the solid line is the semi-analytical for $\bar{I}_4'(1)$.

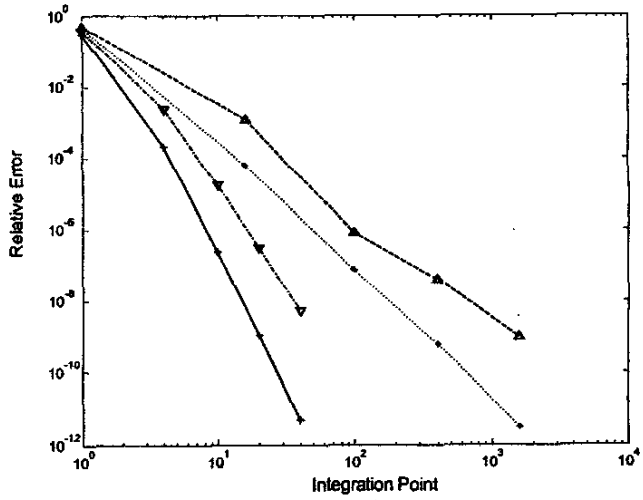

Figure 5b. The maximum relative error for the node-adjacent elements I_3' and $\bar{I}_4'$. The dashed line is the Gaussian quadrature for $I_3'(i=j=1)$; the dashed-dotted line is the semi-analytical for $I_3'(i=j=1)$; The dotted line is the Gaussian quadrature for $\bar{I}_4'(1)$; the solid line is the semi-analytical for $\bar{I}_4'(1)$.

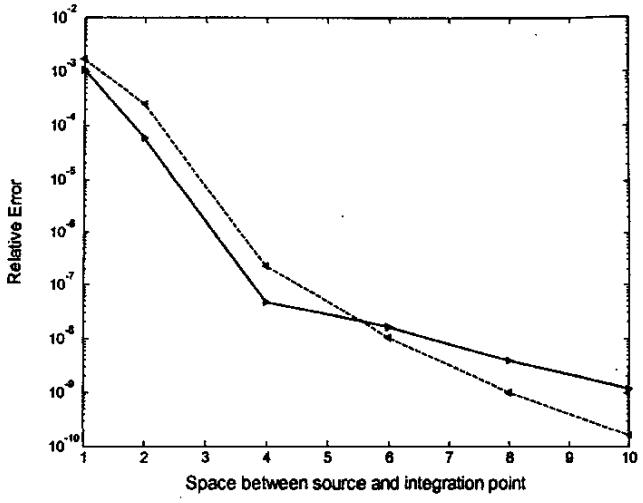

Figure 6. The maximum relative error as a function of the distance between the source and observation elements, based on the semi-analytical expressions. I_1': solid line; $I_3'(i=j=1)$: dashed line.

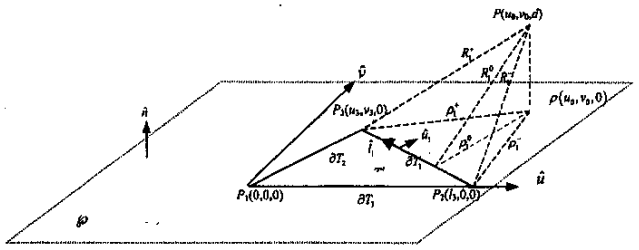

Figure 7. The local geometrical quantities associated with the edge ∂T_1 of the source triangle T' situated in the plane $\wp$. The observation point for the potential is located at $P(u_0, v_0, d)$.

Gaussian quadrature took 4 seconds, i.e., 40 times longer. This significant time saving with the semi-analytical expressions is especially important for the adjacent elements, because they require more integration points to achieve convergence.

Figures 4 and 5 show the comparison of the maximum relative errors for the two pairs of triangles. In both cases, the semi-analytical formulation converged much faster than the Gaussian-quadrature rule. Among the four integrals, $\vec{I}_2'$ and $\vec{I}_4'$ converged slower compared to I_1' and I_3'. Also, it is interesting to see that I_3' and $\vec{I}_4'$ converged faster than I_1' and $\vec{I}_2'$. This suggests that the linear basis function will generate more accurate matrix elements than the constant basis function for nearby elements. As the distance between the observation and source triangle elements increases, fewer integration points are needed to maintain the matrix element accuracy, and this is shown in Figure 6.

4. Conclusion

This paper presented a new semi-analytical expression for evaluating quasi-static double-surface potential integrals occurring in the EFIE. Numerical examples showed that the semi-analytical formulae can improve the accuracy and reduce the computing time rather dramatically when compared to the standard Gaussian-quadrature rules.

5. Acknowledgements

This work was supported by the National Science Foundation under grant no. ECS-01152222. Any opinions, findings, and conclusions or recommendations expressed in this material are those of the authors and do not necessarily reflect the views of the National Science Foundation.

6. Appendix

Analytical Expressions For I_1, $\vec{I}_2$, I_3, and $\vec{I}_4$

Consider the source triangle, T', with the observation point denoted by $P(x,y,z)$, as shown in Figure 7. Using the local coordinates (u,v,n) as defined in Figure 7, the expressions in Equations (12)-(15) can be written in analytical forms based on [2] and [6]. Here, we consider the case when $P \notin T'$. Using the notation in Figure 7, we have

$$I_1(r) = \int_{T'} \frac{1}{R} dT' = -|d|\beta + \sum_{i=1}^{3} \rho_i^0 f_{2i}, \tag{16}$$

$$\vec{I}_2(r) = \int_{T'} \nabla \frac{1}{R} dT' = -\hat{n}\,\mathrm{sgn}(d)\beta - \sum_{i=1}^{3} \hat{u}_i f_{2i}, \tag{17}$$

$$\begin{bmatrix} I_3(r)(i=1) \\ I_3(r)(i=2) \\ I_3(r)(i=3) \end{bmatrix} = \int_{T'} N(\vec{r}') \frac{1}{R} dT'$$

$$= \begin{bmatrix} N_{10} \\ N_{20} \\ N_{30} \end{bmatrix} I_1 + \begin{bmatrix} -1 & u_3/l_3 - 1 \\ 1 & -u_3/l_3 \\ 0 & 1 \end{bmatrix} \begin{bmatrix} I_{ua}/l_3 \\ I_{va}/v_3 \end{bmatrix} \tag{18}$$

$$\vec{I}_4(r) = \int_{T'} N(\vec{r}') \nabla \frac{1}{R} dT'$$

$$= \begin{bmatrix} N_{10} \\ N_{20} \\ N_{30} \end{bmatrix} \vec{I}_2 + \begin{bmatrix} -1 & u_3/l_3 - 1 \\ 1 & -u_3/l_3 \\ 0 & 1 \end{bmatrix} \begin{bmatrix} \vec{I}_{ua}^{\nabla}/l_3 \\ \vec{I}_{va}^{\nabla}/v_3 \end{bmatrix} \tag{19}$$

where

$$\beta = \sum_{i=1}^{3} \left[\tan^{-1} \frac{\rho_i^0 l_i^+}{\left(R_i^0\right)^2 + |d| R_i^+} - \tan^{-1} \frac{\rho_i^0 l_i^-}{\left(R_i^0\right)^2 + |d| R_i^-} \right] \tag{20}$$

$$\begin{bmatrix} I_{ua} \\ I_{va} \end{bmatrix} = \frac{1}{2} \begin{bmatrix} \hat{u} \\ \hat{v} \end{bmatrix} \cdot \sum_{i=1}^{3} \hat{u}_i f_{3i} \tag{21}$$

$$\begin{bmatrix} \bar{I}_{ua}^{\nabla} \\ \bar{I}_{va}^{\nabla} \end{bmatrix} = \hat{n}d \begin{bmatrix} \hat{u} \\ \hat{v} \end{bmatrix} \cdot \sum_{i=1}^{3} \hat{u}_i f_{2i} - \begin{bmatrix} \hat{u} \\ \hat{v} \end{bmatrix} |d| \beta + \sum_{i=1}^{3} \bar{f}_i \begin{bmatrix} \hat{u} \cdot \hat{l}_i \\ \hat{v} \cdot \hat{l}_i \end{bmatrix}_i \qquad (22)$$

N_{i0} $(i = 1,2,3)$ is the value of the ith nodal function evaluated at the point (u_0, v_0),

$$\bar{f}_i = \hat{l}_i \rho_i^0 f_{si} - \hat{u}_i \left(R_i^+ - R_i^- \right), \qquad (23)$$

$$f_{2i} = \ln \left(\frac{R_i^+ + l_i^+}{R_i^- + l_i^-} \right), \qquad (24a)$$

$$f_{3i} = l_i^+ R_i^+ - l_i^- R_i^- + \left(R_i^0 \right)^2 f_{2i}. \qquad (24b)$$

If $d = 0$, it can be shown that $\beta = 0$ when the observation point lies outside the source triangle domain. This further simplifies the above equations. Substituting Equation (5) into Equations (16)-(19), we obtain the analytical formulae for Equations (21)-(24).

As mentioned in [2] and [6], when the observation point is on an edge of T' or its extension, the second term of Equation (16)'s contribution to I_1 vanishes because $\rho_i^0 = 0$. This also applies to Equation (18). However, the authors found that the contribution to Equations (17) and (19) can not be cancelled, since there is no zero term. Below, we develop an expression that overcomes the issue regarding the integrals of Equations (17) and (19), which contain the gradients.

Observation Point Outside the Triangle, But On a Line Through an Edge of the Triangle

For this case (see Figure 8), the observation point, P, is located at the extension of the source triangle edge P_1P_2. Following Graglia [6], when the observation point lies at the positive side of the edge P_1P_2, then

$$\begin{aligned} S_3^- &= -u_0, \\ S_3^+ &= l_3 - u_0, \\ R_3^- &= u_0, \\ R_3^+ &= u_0 - l_3. \end{aligned} \qquad (25)$$

Substituting Equation (25) into Equation (24), we observe that f_{2i} cannot be evaluated, because $\left(R_3^+ + l_3^+ \right) / \left(R_3^- + l_3^- \right) \to 0/0$. However, when the observation point lies on the negative side of the edge P_1P_2, then

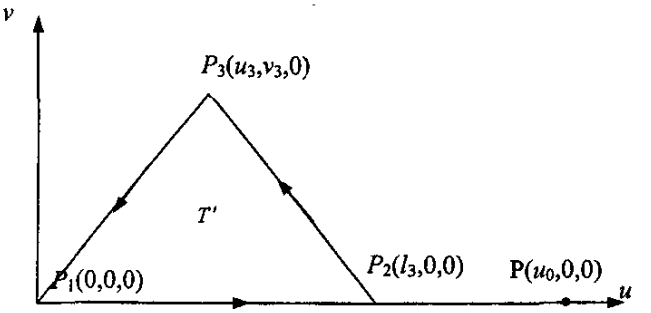

Figure 8. The source triangle, T', with the observation point in the local coordinate frame.

$$\begin{aligned} S_3^- &= u_0, \\ S_3^+ &= l_3 + u_0, \\ R_3^- &= u_0, \\ R_3^+ &= l_3 + u_0. \end{aligned} \qquad (26)$$

In this case, $f_{23} = \ln \left[\left(R_3^+ + l_3^+ \right) / \left(R_3^- + l_3^- \right) \right]$ can be readily evaluated.

To correct the situation when the observation point is to the positive side of one edge of the source triangle, we introduce the expression for the function f_{2i}. This is derived from Equation (24) by setting

$$\begin{aligned} S_3^- &= -u_0, \\ S_3^+ &= l_3 - u_0, \\ R_3^- &= \sqrt{u_0^2 + \Delta\varepsilon^2}, \\ R_3^+ &= \sqrt{(u_0 - l_3)^2 + \Delta\varepsilon^2}, \end{aligned}$$

where $\Delta\varepsilon$ represents a small deviation of the observation point, P, from the u axis. We deduce that

$$f_{23} = \ln \left(\frac{R_3^+ + l_3^+}{R_3^- + l_3^-} \right) = \ln \left(\frac{u_0}{u_0 - l_3} \right); \qquad (27)$$

a numerical example is given below to validate Equation (27). Consider the source triangle $P_1(62.5,25,0)$, $P_2(62.5,25,2)$, $P_3(62.5,37.5,0)$. Table 1 lists the comparison between semi-analytical expressions and the Gaussian quadrature formulae at the observation points $P(62.5,50,0)$ and $P(62.5,0,0)$. In the table, we observe that the values for I_1 and I_3 are unchanged, as

Table 1. Edge effects on $I_1 \sim \bar{I}_4$.

		$I_1(r)$	$\bar{I}_2(r)$	$I_3(r)(i=1,2,3)$	$\bar{I}_4(r)(i=1)$
$P(62.5,50,0)$	Gaussian (7-point)	0.61331767929016	5.62517328324E-19 -3.08494971809E-2 -8.69626496924E-4	0.193075004203650 0.192930866276714 0.227311808729721	1.612329168502E-19 -9.086706817304E-3 -1.939798148981E-4
	Semi-analytic	0.61331767925556	0.000000000000000 -3.08494971540E-2 -8.69626506514E-4	0.193075004247729 0.192930866318881 0.227311808688950	0.0000000000000000 -9.086706830402E-3 -1.939798122746E-4
$P(62.5,0,0)$	Gaussian (7-point)	0.43258463925728	-2.23650927677E-20 1.5102713451293E-2 -3.888703382004E-4	0.149143114990888 0.149057510473345 0.134384013736565	-8.72650566456E-20 5.3719363694375E-3 -1.030046958276E-4
	Semi-analytic	0.43258463925731	0.0000000000000000 1.5102713451304E-2 -3.888703382091E-4	0.149143115010376 0.149057510492870 0.134384013754064	0.0000000000000000 5.3719363694576E-3 -1.030046958380E-4
	Semi-analytic (Ignoring Equation (27))	0.43258463925731	0.0000000000000000 1.5102713451304E-2 *0.405076237769955*	0.149143115010376 0.149057510492870 0.134384013754064	0.0000000000000000 5.3719363694576E-3 *1.21629231962865*

expected. Also, the values of I_2 and I_4 are unchanged for the case $P(62.5,50,0)$. However, for $P(62.5,0,0)$, the z components of $\bar{I}_2$ and $\bar{I}_4$ are significantly in error, unless the new expression for f_{23}, Equation (27), is used.

7. References

1. Paolo Ariconi, Marco Bressan, and Luca Perregrini, "On the Evaluation of the Double Surface Integrals Arising in the Application of the Boundary Integral Method to 3-D Problems," *IEEE Transactions on Microwave Theory and Techniques*, **MTT-45**, March 1997, pp. 436-439.

2. S. M. Rao, R. Wilton, and A W. Glisson, "Electromagnetic Scattering by Surfaces of Arbitrary Shape," *IEEE Transactions on Antennas and Propagation*, **AP-30**, May 1982, pp. 409-418.

3. S. M. Rao, A. W. Glisson, D. R. Wilton, and B. S. Vidula, "A Simple Numerical Solution Procedure for Static Problems Involving Arbitrary-Shaped Surfaces," *IEEE Transactions on Antennas and Propagation*, **AP-27**, September 1979, pp. 604-608.

4. R. F. Harrington, *Field Computation by Moment Methods*, New York, Macmillan, 1968.

5. Donald R. Wilton, S. M. Rao, A. W. Glisson, D. H. Schaubert, O. M. Al-Bundak, and C. M. Butter, "Potential Integrals for Uniform and Linear Source Distributions on Polygonal and Polyhedral Domains," *IEEE Transactions on Antennas and Propagation*, **AP-32**, March 1984, pp. 276-281.

6. R. D. Graglia, "On the Numerical Integration of Linear Shape Functions Times the 3-D Green's Function or its Gradient on a Pane Triangle," *IEEE Transactions on Antennas and Propagation*, **AP-41**, 10, October 1993, pp. 1448-1455.

7. Z. Wang, B. Jensen, J. Volakis, K. Saitou, and K. Kurabayashi, "Analysis of RF-MEMS Switches using Finite Element-Boundary Integration with Moment Method," IEEE International Symposium on Antennas and Propagation *Digest*, **2**, June 22-27, 2003, pp. 173-176.

8. T. F. Eibert and V. Hansen, "On the Calculation of Potential Integrals for Linear Source Distributions on Triangle Domains," *IEEE Transactions on Antennas and Propagation*, **AP-42**, December 1995, pp. 1499-1502.

9. S. Caorsi, D. Moreno, and F. Sidoti, "Theoretical and Numerical Treatment of Surface Integrals Involving the Free-Space Green's Function," *IEEE Transactions on Antennas and Propagation*, **AP-41**, September 1993, pp. 1296-1301.

10. J. L. Volakis, A. Chatterjee, and L. C. Kempel, *Finite Element Method of Electromagnetics*, New York, IEEE Press, 1998.

11. D. Brian, M. Jensen, Zhongde Wang, Kazuhiro Saitou, John Volakis, Katsuo Kurabayashi, "Simultaneous Electrical and Thermal Modeling of a Contact-Type RF MEMS Switch," *2003 ASME International Mechanical Engineering Congress and R&D Expo*, Washington DC, November 15-21, 2003.

12. J. M. Jin, J. L. Volakis, and J. D. Collins, "A Finite Element-Boundary Integral Method for Scattering and Radiation by Two- and Three-Dimensional Structures," *IEEE Antennas and Propagation Magazine*, **33**, 3, June 1991, pp. 22-32.

13. B. D. Jensen, Z. Wang, L. Chow, K. Saitou, K. Kurabayashi, and J. L. Volakis, "Integrated Electrothermal Modeling of RF MEMS Switches for Improved Power Handling Capability," 2003 IEEE Topical Conference on Wireless Communications Technology, October 15-17, 2003, Hawaii.

14. Jin-Fa Lee, R. Lee, and R. J. Burkholder, "Loop Star Basis Functions and a Robust Preconditioned for EFIE Scattering Problems," *IEEE Transactions on Antennas and Propagation*, **AP-51**, August 2003, pp. 1855-1863.

15. B. D. Jensen, K. Saitou, J. L. Volakis, and K. Kurabayashi, "Impact of Skin Effect on Thermal Behavior of RF MEMS Switches," 6th ASME-JSME Thermal Engineering Joint Conference, March 2003, Paper No. TED-AJ03-420.